

# Substitution for Copper in $\text{YBa}_2\text{Cu}_3\text{O}_{9-\delta}$ by 3d- and Pre-transition Metals

Per H. Andresen, Helmer Fjellvåg, Pavel Karen and Arne Kjekshus\*

Department of Chemistry, University of Oslo, Blindern, N-0315 Oslo 3, Norway

Andresen, P. H., Fjellvåg, H., Karen, P. and Kjekshus, A. 1991. Substitution for Copper in  $\text{YBa}_2\text{Cu}_3\text{O}_{9-\delta}$  by 3d- and Pre-transition Metals. – Acta Chem. Scand. 45: 698–708.

The range of solid solubility, as well as structural and superconducting properties, of  $\text{YBa}_2(\text{Cu}_{1-x}\text{M}_x)_3\text{O}_{9-\delta}$  phases ( $M = \text{Li, Mg, Sc, Ti, V, Cr, Mn, Fe, Co, Ni}$  and  $\text{Zn}$ ) have been carefully re-examined for a series of phase-pure samples having high resolution in composition as obtained using citrate gel precursors, mixed at the atomic level. The upper composition limits of the solid solution regimes are  $z_{\text{lim}} = 0.00(3)$  for the elements  $\text{Sc}$  to  $\text{Mn}$ ,  $0.04(1)$  for  $\text{Li}$  and  $\text{Mg}$ , and  $0.22(1)$ ,  $0.30(5)$ ,  $0.08(1)$  and  $0.09(1)$  for  $\text{Fe}$ ,  $\text{Co}$ ,  $\text{Ni}$  and  $\text{Zn}$ , respectively. The phases in equilibrium with  $\text{YBa}_2(\text{Cu}_{1-x}\text{M}_x)_3\text{O}_{9-\delta}$  at the limiting compositions are specified for the different systems, referring to standardized preparation conditions. For oxygen-saturated samples the formal Cu valency (as measured by iodometry) remains constant, and, when permitted, the substituents adopt higher oxidation states, e.g.  $\text{Fe}^{\text{III}}$ ,  $\text{Co}^{\text{III}}$ ,  $\text{Ni}^{>\text{II}}$ . For such samples with  $M = \text{Fe}$  and  $\text{Co}$ , the oxygen content hence may exceed seven. A crossover from orthorhombic to tetragonal symmetry, as seen by powder X-ray diffraction (at 295 K), is studied in detail and occurs at  $z_{\text{O,T}} = 0.030(2)$  and  $0.025(2)$  for  $M = \text{Fe}$  and  $\text{Co}$ , respectively. This behaviour is significantly different from the findings for the substitution of  $\text{La}$  for  $\text{Ba}$  in  $\text{YBa}_2\text{Cu}_3\text{O}_{9-\delta}$ , where the symmetry change is attributed to the linkage in the copper–oxygen chains where the additional oxygens enter. However, when heating orthorhombic samples ( $M = \text{Fe}$  or  $\text{Co}$ ) with composition close to  $z_{\text{O,T}}$ , an increased orthorhombic distortion is induced by thermal removal of oxygen (onset around 570 K), before the symmetry eventually becomes tetragonal at ca. 920 K. All the substituents suppress  $T_c$ , and the suppression is correlated with the degree of tetragonal deformation of the unit cell in terms of the deformation parameter  $D_T = [2c/3(a+b)] - 1$ . No correlation with the orthorhombic distortion parameter  $D_O = (b/a) - 1$  is found.

The physical manifestations of substitution at the various sites in the structure of  $\text{YBa}_2\text{Cu}_3\text{O}_{9-\delta}$  provide important information about parameters which are essential for superconductivity. The extents of the solid solution regions depend on the size, charge and electronic properties of the solute and solvent. However, there is no direct connection between type of structural compatibility and superconductivity. In this respect, significant differences are observed among the four metal sites of  $\text{YBa}_2\text{Cu}_3\text{O}_{9-\delta}$ . Substitution at the Y site does not seem to affect the superconducting properties significantly, regardless of whether the substituent is a rare earth element,<sup>1</sup>  $\text{Bi}^2$  or  $\text{Ca}$ .<sup>3–5</sup> This supports the idea that superconductivity in this class of materials is confined to the copper–oxygen structural network.<sup>6</sup> The substitution for Ba by smaller elements, such as La or Sr, affects the superconductivity more profoundly and is accompanied by significant changes in some of the Cu–O interatomic distances.<sup>7–10</sup> The third option for studying the relationship between superconductivity and structure is to perturb the local structural and electronic environment at one or both of the Cu sites.

The Cu sites are reported to host a large variety of substituents, including  $\text{Mg}$ ,<sup>11</sup>  $\text{Al}$ ,<sup>12–14</sup>  $\text{Ga}$ ,<sup>15–18</sup>  $\text{Ti}$ ,<sup>19</sup>  $\text{V}$ ,<sup>19</sup>  $\text{Cr}$ ,<sup>19,20</sup>  $\text{Mn}$ ,<sup>19,21</sup>  $\text{Fe}$ ,<sup>22–27</sup>  $\text{Co}$ ,<sup>28–33</sup>  $\text{Ni}$ ,<sup>30,32,34–36</sup>  $\text{Pd}$ ,<sup>37</sup>  $\text{Ag}$ ,<sup>19</sup>  $\text{Au}$ ,<sup>38</sup>  $\text{Zn}$ <sup>14,17,30,39–42</sup> and  $\text{Cd}$ .<sup>42</sup> However, the differences in sample characteristics stemming from the different goals of the cited studies make any consequent comparisons between chemical, structural and superconductivity features difficult. In particular, proper checks on phase purity and oxygen content analyses have not been consistently presented. Furthermore, the limits of solid solubility are usually not stated, and it is unclear whether the miscibility limits have been considered during measurements of physical properties. In this study, a comparison between structural and superconducting properties is presented for well characterized  $\text{YBa}_2(\text{Cu}_{1-x}\text{M}_x)_3\text{O}_{9-\delta}$  samples, where  $M = \text{Li, Mg, Sc, Ti, V, Cr, Mn, Fe, Co, Ni}$  and  $\text{Zn}$ .

## Experimental

**Syntheses.** The samples were prepared by multiple firing of precursors obtained by liquid mixing in citrate gels. The components, viz.  $\text{Y}_2\text{O}_3$  (5 N, Megon),  $\text{BaCO}_3$  (reagent grade, Merck) and  $\text{CuCO}_3 \cdot \text{Cu}(\text{OH})_2 \cdot 0.5\text{H}_2\text{O}$  (*puriss.*,

\* To whom correspondence should be addressed.

Riedel de Häen), were dissolved in boiling citric acid monohydrate (reagent grade, Fluka). A clear blue citrate solution was obtained after adding water to twice the original volume. The substituent was then added, either in a water-soluble form or in solution. The citrate gel, formed upon evaporation of the solvent, was dried at 180 °C, incinerated in air, milled, pelletized and subsequently fired for 20 h at 910 °C in a corundum boat under a flow of purified oxygen, before being finally oxidized at 340 °C for 16 h. The firing procedure was repeated twice, with intermediate rehomogenizations in an agate ultrafine vibration mill. Complete and reproducible oxidation was ensured using loosely pressed pellets of a coarsely powdered product in the final heat treatment.

The following compounds were used as sources for the substituents:  $\text{Li}_2\text{CO}_3$  (reagent grade, Merck); basic magnesium carbonate (reagent grade, Merck, magnesium content analyzed volumetrically using  $\text{Na}_3\text{HEDTA}$  and Eriochrom Black T indicator at pH 10);  $\text{Sc}(\text{HCOO})_3$  (6 N purity, according to ICP emission spectral analysis); ammonium titanil oxalate (Specpure, Johnson Matthey; Ti was analyzed gravimetrically as  $\text{TiO}_2$ , and used as a citrate- and peroxide-complexed solution, obtained upon boiling 1 g of ammonium titanil oxalate with 5 g citric acid, 5 ml water and 2 ml 40%  $\text{H}_2\text{O}_2$ );  $\text{NH}_4\text{VO}_3$  (reagent grade, Merck);  $\text{CrO}_3$  (reagent grade, Merck);  $\text{MnCO}_3$  (reagent grade, Merck, Mn content analyzed in a solution stabilized with hydroxylammonium chloride and trimethylene glycol using the same method as for Mg); Fe powder (reagent grade, Merck, used as a citrate solution after dissolution in excess citric acid during heating);  $\text{Co}(\text{COO})_2 \cdot 6\text{H}_2\text{O}$  (reagent grade, BDH, used after dissolution in warm, concentrated nitric acid);  $\text{Ni}(\text{NO}_3)_2 \cdot 6\text{H}_2\text{O}$  (reagent grade, J. T. Baker);  $\text{Zn}(\text{C}_2\text{H}_3\text{O}_2)_2 \cdot 2\text{H}_2\text{O}$  (reagent grade, Merck).

*Oxygen content analyses.* The oxygen content in the products was determined iodometrically. The analysis is based on comparison of the total oxidative force of the solid as such with that of  $\text{Cu}^{2+}$  obtained after reduction of the solid with HCl. The prerduced  $\text{Cu}^{2+}$  solution was obtained by dissolving ca. 0.15 g of the sample in ca. 20 ml 1 M HCl. The solution was thereafter evaporated until the appearance of crystals, and then redissolved in water. The iodine released after adding ca. 1 g KI in 20 ml water was titrated by 0.1 M  $\text{Na}_2\text{S}_2\text{O}_3$ . Before the end point, 2 ml of a 10% solution of  $\text{NH}_4\text{SCN}$  were added, and the exact end point was determined by means of a soluble starch indicator. In order to determine the total oxidative power, ca. 0.1 g of a finely milled sample was first suspended in a solution of ca. 1 g KI in 20 ml water, the flask was then filled with Ar and 8 ml of 1 M HCl were added. After ca. 1 h (with occasional stirring), the released iodine was titrated. The accuracy of the determinations is, in units of the formal oxidation state of copper,  $\pm 0.01$ .

In specific cases, precautions were taken to ensure a specific oxidation state of the substituents during a particular step of the analysis. The presence of  $\text{V}^{\text{IV}}$  in the acid

prerduced portion was ensured by prolonged boiling with hydrochloric acid ( $\text{Cu}^{2+}$  catalyzed reduction),<sup>43</sup> while  $\text{V}^{\text{IV}}$  forms readily<sup>44</sup> during the reaction with iodide. Similarly,  $\text{Mn}^{\text{II}}$  was obtained during prolonged heating with HCl and subsequently stabilized by complexing with triethylene glycol. The thiosulphate titration was performed immediately afterwards.  $\text{Fe}^{\text{III}}$  in both the HCl and iodide reduced portions was stabilized by complexing using 10 mol of  $\text{Na}_4\text{P}_2\text{O}_7$  per mol of Fe. The acidity was subsequently adjusted by 1 M HCl prior to the titration reaction.

*Powder X-ray diffraction.* All samples were checked for homogeneity and characterized by powder X-ray diffraction (PXD). Guinier Hagg cameras,  $\text{CuK}\alpha_1$  radiation and Si as internal standard were used. High-temperature PXD patterns were obtained at temperatures between 100 and 1000 °C using a Guinier Simon camera (Enraf-Nonius) and  $\text{CuK}\alpha_1$  radiation. The samples were placed in open silica capillaries and heated at a rate of 50 °C  $\text{h}^{-1}$ . Position and intensity measurements of the reflections were carried out using a Nicolet L18 film scanner controlled by the SCANPI program<sup>45</sup> system. Unit cell parameters were obtained by least-squares refinements using the CELLKANT program.<sup>46</sup> Quantitative estimates of phase contents were based on comparisons of PXD intensities of the samples with those of standard mixtures.

*Low-temperature magnetic susceptibility.* The a.c. induction method was adopted for the determination of  $T_c$  and of the degree of Meissner effect ( $T > 56$  K). A pulverized sample (50 mg) was placed into a cylindrical ( $l/r \approx \sqrt{3}$ ) sample holder in a closed chamber inside a field coil (4.4 kOe, 300 Hz) and cooled by liquid nitrogen. The voltage induced in the pick-up coils was registered by a lock-in voltmeter. The temperature was measured by a type-T, Cu-Cu/Ni thermocouple in contact with the sample. The Meissner effect was determined as an absolute value of dimensionless diamagnetic susceptibility, expressed as a percentage. An apparent density of the powder sample of 3  $\text{g cm}^{-3}$  was used to calculate the susceptibility per unit volume. Dysprosium oxide was used to calibrate the (paramagnetic) susceptibility reading. Magnetic susceptibility data for temperatures between 56 and 2 K were obtained by a SQUID magnetometer (Quantum Design). The transition temperature  $T_c$  was determined as the temperature with 1% remaining Meissner effect.

## Results and discussion

*Formation and composition limits of  $\text{YBa}_2(\text{Cu}_{1-z}\text{M}_z)_3\text{O}_{9-\delta}$  solid solutions.* For the solid solution phases in question, there are two compositional variables. One variable,  $z$ , concerns both of the two non-equivalent Cu sites, the other,  $\delta$ , concerns the oxygen sites in the Cu-O chains. Since the substitution behaviour at each of the two Cu sites is different, a more informative formula would be  $\text{YBa}_2\text{Cu}_{1-m}\text{M}_m(\text{Cu}_{1-n}\text{M}_n)_2\text{O}_{9-\delta}$ , with  $(m + 2n)/3 = z$ .

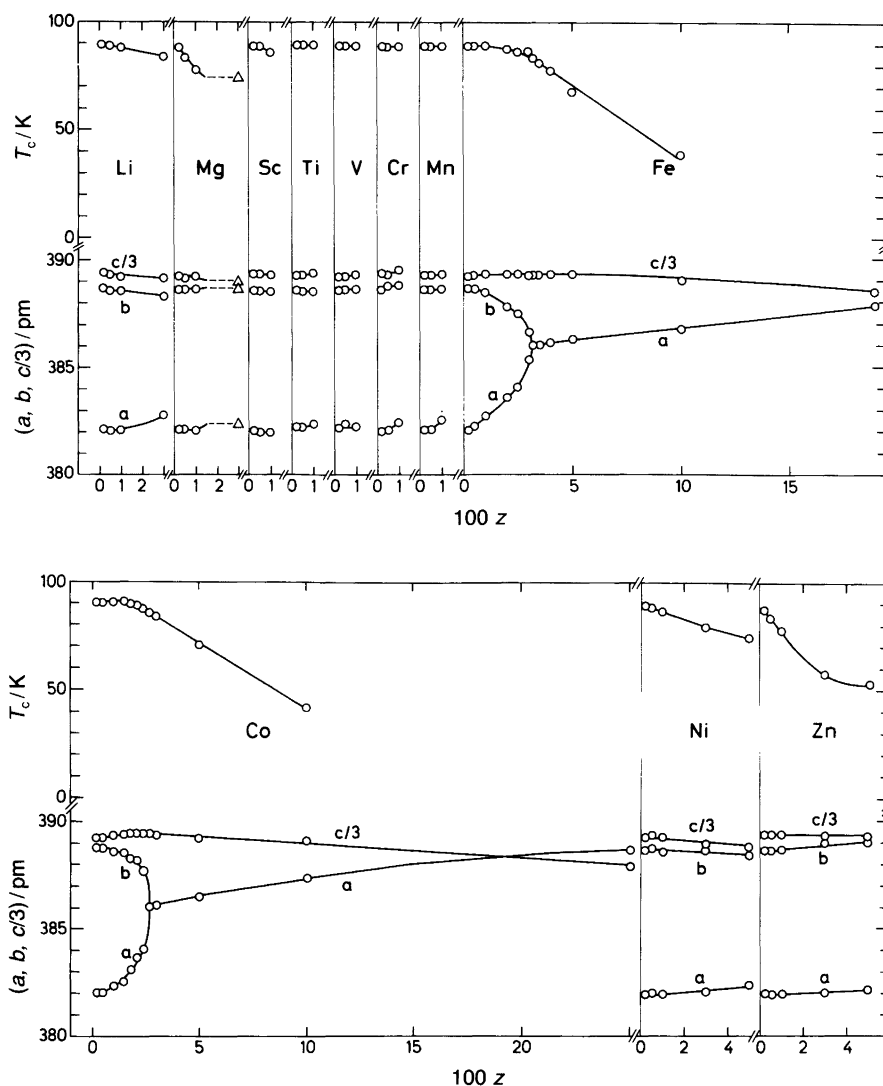


Fig. 1. Unit cell parameters and onset of superconductivity  $T_c$  for oxygen-saturated  $\text{YBa}_2(\text{Cu}_{1-z}\text{M}_z)_3\text{O}_{9-\delta}$ ;  $M = \text{Li, Mg, Sc, Ti, V, Mn, Cr, Fe, Co, Ni}$  and  $\text{Zn}$ . The size of the circles exceeds three standard deviations as calculated (unit cell parameters) or as estimated ( $T_c$ ).

The ability of the Cu sites to accommodate 3d-transition metals, Mg or Li, varies significantly among these substituents. Practically zero substitution is found for the early d-transition metals (Fig. 1 and Table 1). However, since the detection threshold for the presently used high-sensitivity PXD instrumentation is 0.5 and 1 wt % for (the nearest-neighbouring phases)  $\text{Y}_2\text{BaCuO}_5$  and  $\text{BaCuO}_{2+v}$ , respectively, a substitution limit below  $z = 0.01$  could not be ascertained. Based on the quantitative phase analyses, the limits of solid solubility were calculated by mole-balances, and are given in Table 1, together with a list of the identified equilibrium phases at the verge of the solid solution regime.  $M = \text{Fe}$  and  $\text{Co}$ , which have the highest solid solubility limits, give rise to the quinary oxide  $\text{YBaCuMO}_5$ , the structure of which follows from that of  $\text{YBa}_2\text{Cu}_3\text{O}_{9-\delta}$  by removing the Cu(1) square chains, together with half of the neighbouring Ba atoms. A ternary

$\text{Ba}_2\text{M}$  oxide is formed in addition.  $M = \text{Li, Mg, Ni}$  and  $\text{Zn}$ , showing intermediate solubility, emerge as oxides  $\text{MO}$  ( $M = \text{Li}$  apparently as a carbonate) and tend to substitute partially  $\text{BaCuO}_2$  and  $\text{Y}_2\text{BaCuO}_5$  formed simultaneously [note that these are neighbours to  $\text{YBa}_2\text{Cu}_3\text{O}_{9-\delta}$  in the  $\text{Y}(\text{O})\text{-Ba}(\text{O})\text{-Cu}(\text{O})$  phase diagram].  $M = \text{Sc-Mn}$ , with the lowest solubility, appear as Ba 'salts',\* consistent with their readiness to form relatively acidic oxides. The final balance is taken care of here by the simultaneous formation of  $\text{Y}_2\text{BaCuO}_5$ .

The solubility limits of the various substituents (Table 1) agree reasonably well with the sparse data explicitly stated

\*Ti forms a series of ternary barium oxides which are mutually close in composition, and several of these oxides occur in the phase mixtures as an apparent consequence of their inability to reach equilibrium under the present, very dilute conditions.

Table 1. Equilibrium phase composition at the limit of solid solubility ( $z_{\text{lim}}$ ) for  $M$  in  $\text{YBa}_2(\text{Cu}_{1-z}M_z)_3\text{O}_{9-\delta}$  for samples fired at 910 °C and oxidized at 340 °C.

$M$	$\text{Y}_2\text{BaCuO}_5$	$\text{BaCuO}_{2+v}$	Other observed phases	$z_{\text{lim}}$
Li	+	+	$\text{BaCO}_3(\cdot \text{Li}_2\text{CO}_3 ?)$	0.04(1)
Mg	+	+	MgO	0.04(1)
Sc	+	–	$\text{BaSc}_2\text{O}_4^a$	0.01(1)
Ti	+	–	$\text{Ba}_2\text{TiO}_3$ , $\text{BaTi}_2\text{O}_5$ , $\text{BaTi}_4\text{O}_9$ , $\text{TiO}_2$	0.00(2)
V	+	–	$\text{Ba}_3\text{V}_2\text{O}_8^a$	0.00(4)
Cr	+	–	$\text{BaCrO}_4^a$	0.02(1)
Mn	+	–	$\text{Ba}_3\text{Mn}_2\text{O}_8^a$	0.00(3)
Fe	–	+ <sup>b</sup>	$\text{YBa}(\text{Cu}_{1-z}\text{Fe}_z)_2\text{O}_5^c$	0.22(1)
Co	–	–	$\text{YBa}(\text{Cu}_{1-z}\text{Co}_z)_2\text{O}_5^d$ ; $\text{Ba}_3(\text{Co}_{1-z}\text{Cu}_z)_2\text{O}_w^{a,e}$	0.30(5)
Ni	+ <sup>f</sup>	+ <sup>f</sup>	NiO	0.08(1)
Zn	+ <sup>f</sup>	+ <sup>f</sup>	<sup>a</sup>	0.09(1)

<sup>a</sup>A small amount of an additional phase is expected to occur. <sup>b</sup> $\text{Ba}(\text{Cu}_{0.70(5)}\text{Fe}_{0.30(5)})\text{O}_{2+v}$  with  $a = 1842.4(4)$  pm, iron content from Vegard's rule and a set of standard solid solution samples. <sup>c</sup>Tetragonal,  $a = 387.0(1)$ ,  $c = 767.1(1)$  pm;  $z$  approaching 0.50 since  $a = 386.88(3)$ ,  $c = 766.21(9)$  pm for phase-pure  $\text{YBaCuFeO}_5$ . <sup>d</sup>Tetragonal,  $a = 387.2(1)$ ,  $c = 756.2(2)$  pm;  $z$  approaching 0.50 since  $a = 387.02(2)$ ,  $c = 756.80(6)$  pm for phase-pure  $\text{YBaCuCoO}_5$ . <sup>e</sup>Hexagonal,  $a = 571.65(2)$ ,  $c = 444.00(2)$  pm;  $z$  close to 0.00 since  $a = 570.94(3)$ ,  $c = 447.68(4)$  pm for phase-pure  $\text{Ba}_3\text{Co}_2\text{O}_{7.13(3)}$ . <sup>f</sup>Ni for Cu and Zn for Cu substitutions occur according to mole-balance calculations.

in the literature, e.g. Fe (18 %<sup>23</sup>), Co (25 %<sup>33</sup>), Ni (4;<sup>47</sup> 9;<sup>34</sup> 10–17 %<sup>35</sup>) and Zn (10 %;<sup>14</sup> 12 %<sup>48</sup>).

The second compositional variable of the  $\text{YBa}_2(\text{Cu}_{1-z}M_z)_3\text{O}_{9-\delta}$  solid solutions, *viz.* the oxygen content, is usually affected by  $M$ . For these solid solutions, the iodometric titration used for the analysis of the oxygen content gives a *sum* of the oxidation numbers of Cu plus  $M$  in the solid (provided the valency,  $\nu_M$ , of  $M$ , stabilized in the iodide-containing solution after the titration, is defined). As a consequence, while the oxygen content is unequivocally established, either  $\nu_{\text{Cu}}$  or  $\nu_M$  in the solid state must be known or estimated in order to specify the particular valence states. An overview of the results of the iodometric titrations is provided in Table 2. In the trivial case that  $M$  has only one valence state (e.g. Li, Mg or Zn), the formal  $\nu_{\text{Cu}}$  may be calculated directly, and is found to be roughly constant for the oxygen-saturated samples. Since  $\nu_M$  for  $M = \text{Li}$ , Mg or Zn is lower than the formal average valence of Cu, the oxygen content  $9 - \delta$  decreases with increasing  $z$  in  $\text{YBa}_2(\text{Cu}_{1-z}M_z)_3\text{O}_{9-\delta}$ . Also for  $M = \text{Fe}$ , when  $\text{Fe}^{\text{III}}$  is presumed to be in the solid state, the formal copper valency is found to be roughly constant. A virtually unchanged formal copper valency is also found for the substitutions of  $\text{La}^{\text{III}}$  for Ba or  $\text{Ca}^{\text{II}}$  for Y. These facts justify the generalization that the formal copper valency remains roughly constant upon substitutions by the 3d- and pre-transition metals, at, say,  $\nu_{\text{Cu}} = 2.29(2)$ , as listed in Table 2 for the substituted samples with fixed  $\nu_M$ . From this semi-postulated constant  $\nu_{\text{Cu}}$ , the formal oxidation states are calculated to be almost III for  $M = \text{Co}$  and  $> \text{II}$  for  $M = \text{Ni}$  (Table 2).

The high oxidation states adopted by the polyvalent substituents agree with earlier findings obtained by different analytical,<sup>32</sup> structural<sup>24,49</sup> and spectroscopic<sup>27,50–52</sup> methods, although some data<sup>33,53</sup> are apparently erroneous. Since the

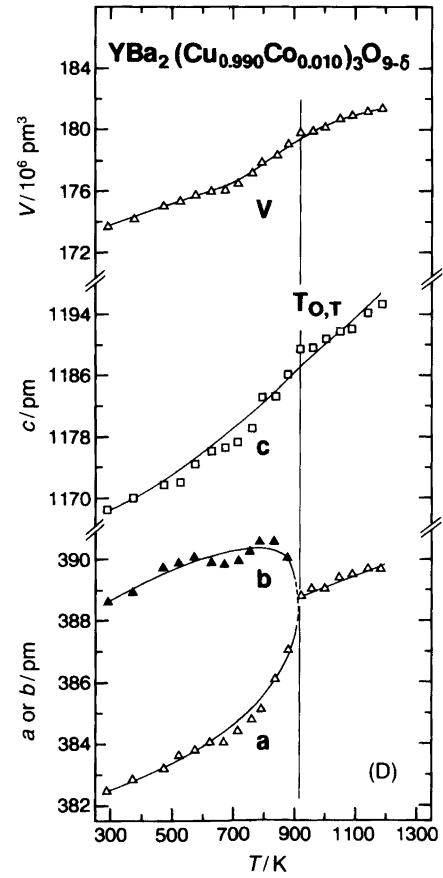
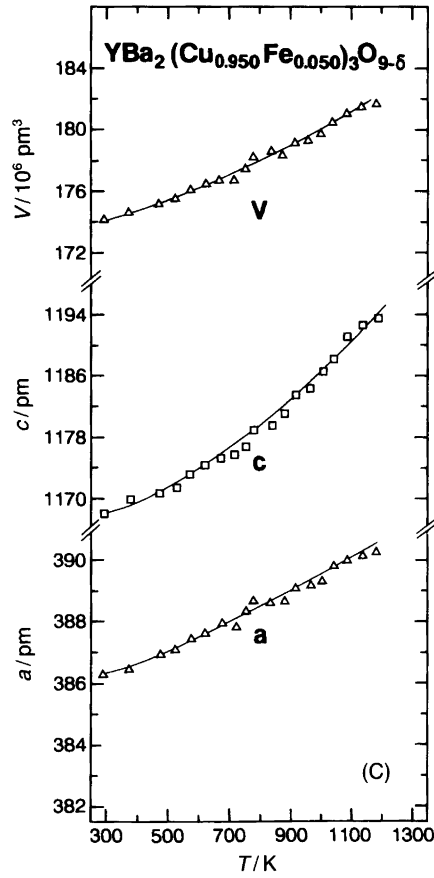
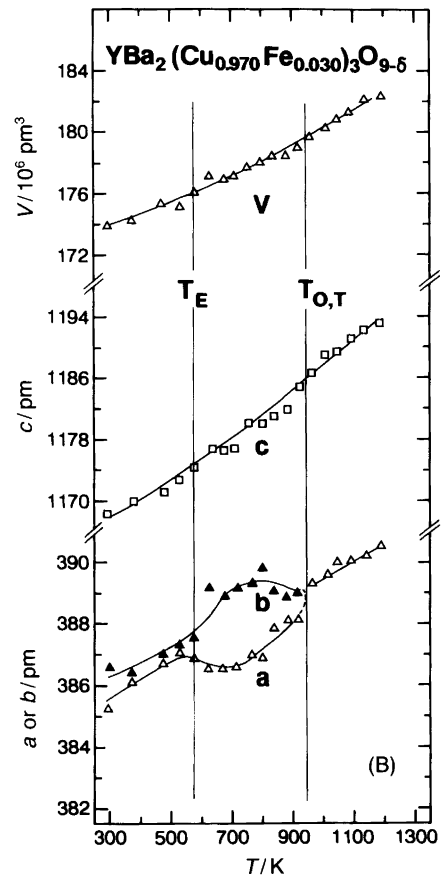
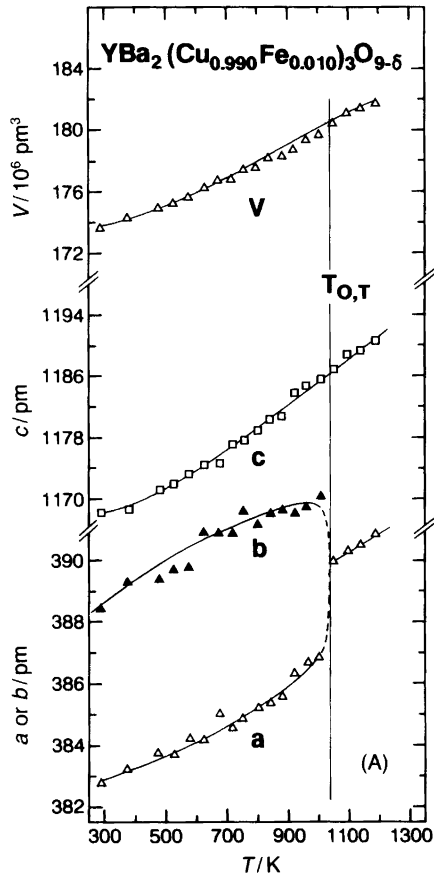
formal oxidation state of Cu is lower than that of Fe, Co and Ni, an increase in oxygen content is observed upon substitution. For high substitution levels of Fe and Co, this means that the equilibrium oxygen content exceeds  $9 - \delta = 7$  (for samples saturated at 340 °C in 1 atm  $\text{O}_2$ ).

*Structural properties of  $\text{YBa}_2(\text{Cu}_{1-z}M_z)_3\text{O}_{9-\delta}$ .* The metric of the unit cell at room temperature (Fig. 1) is adopted here as a basis for comparisons of the structural effects due to substitutions at the Cu sites, since detailed atomic position coordinates are not available in the literature for all sub-

Table 2. Oxygen content and valencies  $\nu_{\text{Cu}}$  and  $\nu_M$  for samples of  $\text{YBa}_2(\text{Cu}_{1-z}M_z)_3\text{O}_{9-\delta}$  fired at 910 °C and oxidized at 340 °C.<sup>a</sup>

$M$	$z$	$\nu_{M,\text{sol}}$	$\nu_M$	$\nu_{\text{Cu}}$	$9 - \delta$
Li	0.01	I	I	2.305	6.94
	0.03			2.311	6.91
Mg	0.01	II	II	2.273	6.91
	0.03			2.260	6.88
Fe	0.03	III	III	2.282	6.96
	0.05			2.297	7.00
	0.10			2.302	7.06
Co	0.05	II	2.8(4)	2.29(2)	6.97
	0.10		2.9(2)	2.29(2)	7.03
	0.25		2.93(6)	2.29(2)	7.18
Ni	0.03	II	2.9(7)	2.29(2)	6.96
	0.05		2.6(4)	2.29(2)	6.96

<sup>a</sup>Formal copper valency,  $\nu_{\text{Cu}}$ , is calculated from iodometric analyses; for  $M = \text{Co}$  and Ni  $\nu_{\text{Cu}}$  is assumed equal to the average of previous values, see text. Valencies for  $M = \text{Li}$ , Mg and Fe are postulated. Stabilized valencies during iodometric titrations,  $\omega_{M,\text{sol}}$  are included. Estimated uncertainties are given in parentheses.



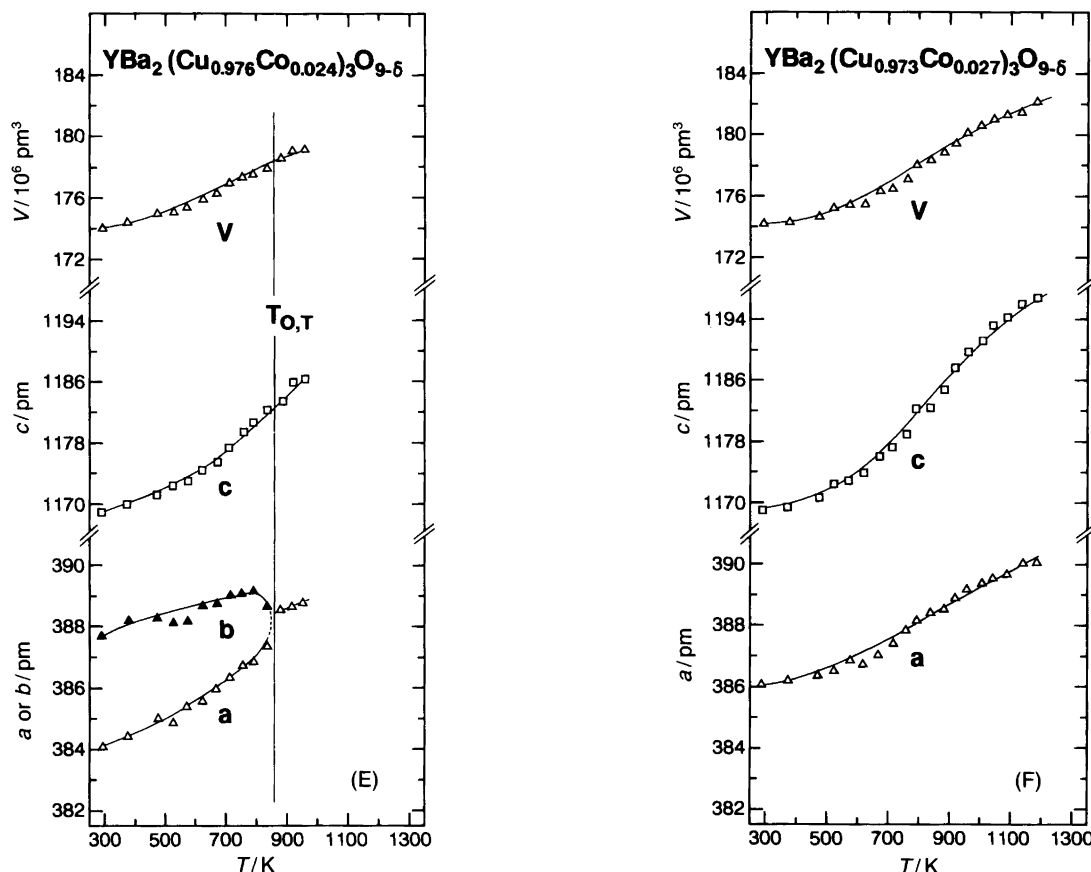


Fig. 2. Temperature variation of unit cell parameters of oxygen-saturated  $\text{YBa}_2(\text{Cu}_{1-z}\text{M}_z)_3\text{O}_{9-\delta}$  between 300 and 1250 K in air: (A)–(C)  $M = \text{Fe}$ ; (D)–(F)  $M = \text{Co}$ ; compositions are given on the illustrations. The size of symbols reflects estimated standard deviations.

stituents across the entire solid solution regime. No significant changes in the unit cell parameters are observed for samples substituted by Mg, Sc, Ti, V, Cr and Mn, whereas the substitutions by Li and Fe – Zn are well manifested in the unit cell metric.

The substituents Fe, Co and Zn increase the unit cell volume, whereas Ni decreases it. A special feature of the Fe and Co substitutions is that they rapidly lead to tetragonal symmetry (as observed by PXD). This behaviour coincides with the substitution of  $\text{Fe}^{\text{III}}$  and  $\text{Co}^{\text{III}}$  at the Cu(1) site (square chains),<sup>24,30,49</sup> where they exert a tendency for non-planar coordination (tetrahedral for iron<sup>54</sup> or octahedral for cobalt<sup>52</sup>). These substituents therefore tend to concentrate at the twin-domain boundaries. At the substitution level  $z_{\text{O,T}}$ , where the change in crystal symmetry occurs, nanoscopic orthorhombic domains are observed by HREM,<sup>52,55</sup> but naturally not by diffraction methods. However, either as a consequence of the still relatively large size of the domains, or due to the distribution of the substituent within or among grains, a broadening of the Bragg reflections is observed close to the transitional concentrations. [Inhomogeneities corresponding to  $\Delta z = \pm 0.01$  (ca. 90% probability level) are reported according to electron micro-

probe analysis after the first firing of a substituted sample.<sup>56</sup>] The transitional substitution levels were evaluated from samples with close, but well resolved composition, and are  $z_{\text{O,T}} = 0.030(2)$  for  $M = \text{Fe}$  and  $z_{\text{O,T}} = 0.025(2)$  for  $M = \text{Co}$  (samples saturated in 1 atm  $\text{O}_2$  at 340°C).

It is interesting to recall that the orthorhombic structure persists<sup>57,58</sup> at even higher substitution levels of iron (and cobalt) if a reducing atmosphere is applied at the firing temperature and the following reoxidation is performed at low temperatures.<sup>57,58</sup> Instead of the Cu(1) site, the square-pyramidal Cu(2) site is supposed<sup>57,58</sup> to host the iron in the reduced samples. Indeed an increase in  $n$  is observed<sup>59</sup> in such samples of  $\text{YBa}_2\text{Cu}_{1-m}\text{M}_m(\text{Cu}_{1-n}\text{M}_n)_2\text{O}_{9-\delta}$ , where, for example,  $m \approx 0.14$  and  $n \approx 0.08$  is found by Mössbauer spectroscopy, as compared to  $m \approx 0.24$  and  $n \approx 0.03$  for the samples prepared in oxygen. It is feasible that the high-temperature, tetragonal structure (i.e. with no twinning) favours a random distribution of Fe at the Cu(1) site. This may be ‘frozen in’ upon cooling in the absence of oxygen. At low temperatures, where the diffusion of the oxygen is essential for the formation of the oxidized orthorhombic phase, the diffusion of the substituent atoms is very slow, and thus the formation of twin nanodomain borders may

well be hindered. In this case, the substituent-induced change to a tetragonal structure occurs at approximately the same concentration (and for the same reasons) as when La is substituted for Ba,<sup>8</sup> viz. as a consequence of the accommodation of additional oxygens at the sites octahedrally adjacent to the Cu–O square chains.

Li-substituted samples show only a minor tendency towards diminishing orthorhombic distortion, which is consistent with the inference<sup>60</sup> that Li statistically occupies both the Cu(1) and Cu(2) sites.

Mg, Ni and Zn as substituents are supposed<sup>48,61–63</sup> to be accommodated predominantly at the Cu(2) site. In these cases the structure remains orthorhombic throughout the entire solid solution regimes.

All substituted samples show a nonlinear thermal expansion, as determined by PXD. For  $M = \text{Fe}$  and  $\text{Co}$ , the high-temperature behaviour is considered to be of particular interest, and the variations of the unit cell parameters with temperature for selected samples are shown in Figs. 2(A)–(F), respectively. As is the case for the  $\text{YBa}_2\text{Cu}_3\text{O}_{9-\delta}$  parent compound, the initially orthorhombic samples show a thermally induced transition into tetragonal symmetry at the temperature  $T_{\text{O,T}}$ . The transition temperature decreases only slightly when the substitution level approaches the transitional concentration  $z_{\text{O,T}}$ . As an example,  $T_{\text{O,T}}$  decreases from 950 K for  $z = 0.000$  to 900 and 860 K for  $M = \text{Co}$  with  $z = 0.010$  and 0.024, respectively, whereas it remains virtually constant for the  $M = \text{Fe}$  samples.

In the region very close to  $z_{\text{O,T}}$  (e.g. for  $M = \text{Fe}$ ,  $z = 0.030$ ) the almost tetragonal samples (with broadened PXD reflections) undergo an enhanced orthorhombic distortion upon heating, starting at the temperature  $T_E = 550$  K, which corresponds to the onset of the thermal release of oxygen.<sup>64</sup> Analogous high-temperature behaviour is observed for  $\text{Y}(\text{Ba}_{1-y}\text{La}_y)_2\text{Cu}_3\text{O}_{9-\delta}$ , where the aliovalent La substitution also allows additional oxygens to enter the structure.<sup>8</sup> Samples with substitution levels higher than  $z_{\text{O,T}}$  show a smooth expansion of their tetragonal unit cells over the entire temperature range 300–1200 K, cf. Figs. 2(C) and (F).

**Superconducting properties of  $\text{YBa}_2(\text{Cu}_{1-z}\text{M}_z)_3\text{O}_{9-\delta}$ .** An overview of the superconducting and structural properties of the substituted samples is provided in Fig. 1. Generally, all substitutions for Cu (cf. Table 1 for substitution limits) are accompanied by a decrease in  $T_c$ . No change was found in  $T_c$  for  $M = \text{Ti}$ ,  $\text{V}$ ,  $\text{Cr}$  and  $\text{Mn}$ , but in these cases negligible solid solubility was indicated by PXD and chemical analyses. Using criteria of both a qualitative (the shape of the  $T_c$  versus  $z$  relation) and a quantitative nature [graphic differentiation of the  $T_c(z)$  function], the remaining substituents may be divided into three groups according to their effect on the value of  $T_c$ : (i) Substituents causing a rapid decrease of  $T_c$ . Zn and Mg serve as examples.  $dT_c/dz \approx -1200$  K at  $z = 0.005$ . (ii) Substituents causing an initially slow, later intermediate decrease of  $T_c$ . Fe and Co

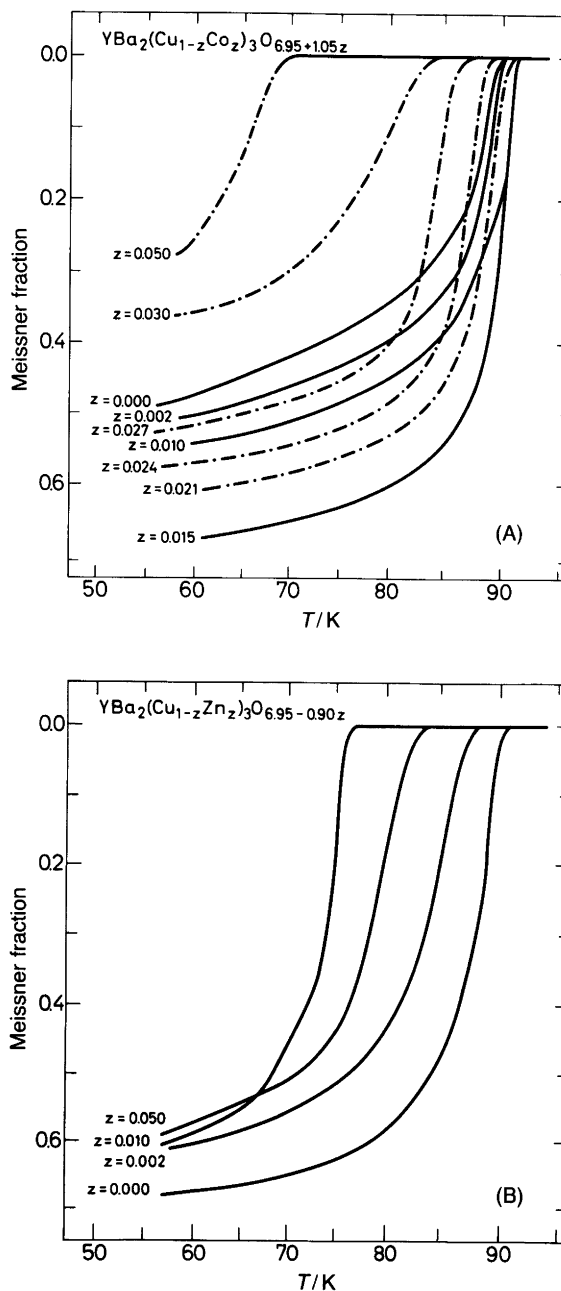


Fig. 3. Diamagnetic susceptibility (Meissner fraction) for oxygen-saturated  $\text{YBa}_2(\text{Cu}_{1-z}\text{M}_z)_3\text{O}_{9-\delta}$  as a function of temperature: (A)  $M = \text{Co}$ ; (B)  $M = \text{Zn}$ .

serve as examples, with  $dT_c/dz \approx -800$  K at  $z \approx 0.05$ . (iii) Substituents causing a minor change in  $T_c$ .  $T_c(z)$  remains close to linear. Ni, with  $dT_c/dz \approx -400$  K, and Li, with  $dT_c/dz \approx -200$  K, belong to this category.

Before further discussion of  $T_c$  as a function of  $z$  in  $\text{YBa}_2(\text{Cu}_{1-z}\text{M}_z)_3\text{O}_{9-\delta}$ , an appropriate question to address is whether or not the measured Meissner effect is connected with possible inhomogeneities in the samples. The Meissner fractions were calculated from the susceptibilities obtained from powder samples at 60 K. Under these condi-

tions, ca. 50% of the Meissner effect is observed for the parent compound. Upon the substitutions, no sudden drops or 'tails' in the Meissner effect versus  $T_c$  curves are observed, the Meissner effect decreasing smoothly and proportionally with the lowering in  $T_c$  as a consequence of enhanced flux creep. The observed variations of the Meissner effect with  $z$  are well reproducible.

As examples, the measured a.c. susceptibility curves for Co and Zn substitution are shown in Figs. 3(A) and (B). The anomalous increase in  $T_c$  and in the Meissner effect observed at the low Co substitution levels around  $z = 0.01$  may be compared with the 'normal' behaviour found in the case of Zn substitution. In Fig. 4 the relative variations in the Meissner effect are shown as functions of the number of rehomogenizations for the samples with low Co contents. A different (random) variation is observed among the different samples, but the variation for a given sample is consistent (Fig. 4), and the original differences among the samples (Fig. 5) are preserved. Similar trends are observed for  $T_c$ . Based on Fig. 4, it may be judged that the substituted samples are single phase with a reasonably homogeneous distribution of the solute over the entire sample, even at low concentrations.

It is therefore reasonable to presume that there are reproducible correlations between the observed variation in  $T_c$ , the concentration of the substituent  $M$ , and other, relevant properties of  $\text{YBa}_2(\text{Cu}_{1-z}\text{M}_z)_3\text{O}_{9-\delta}$ . In principle,  $T_c$  should be correlated with the electronic band structure.

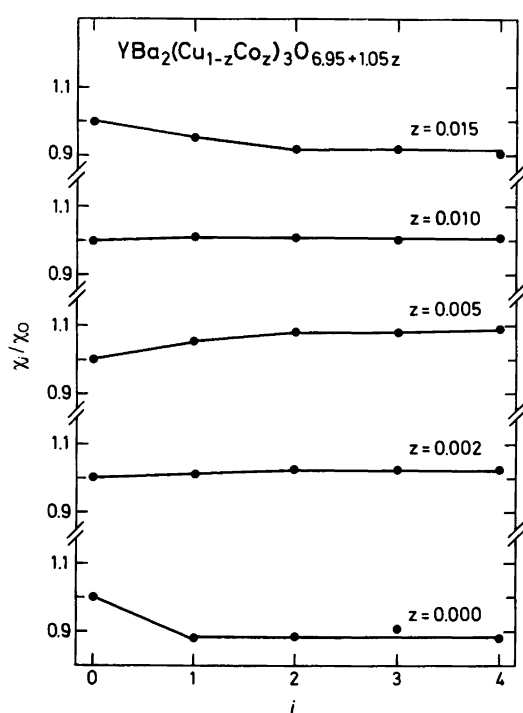


Fig. 4. Relative change in Meissner fraction at 60 K for  $\text{YBa}_2(\text{Cu}_{1-z}\text{Co}_z)_3\text{O}_{6.95+1.05z}$  for low concentrations, as a function of the number ( $i$ ) of rehomogenizations (milling, 40 h annealing at 900 °C and oxygen saturation).

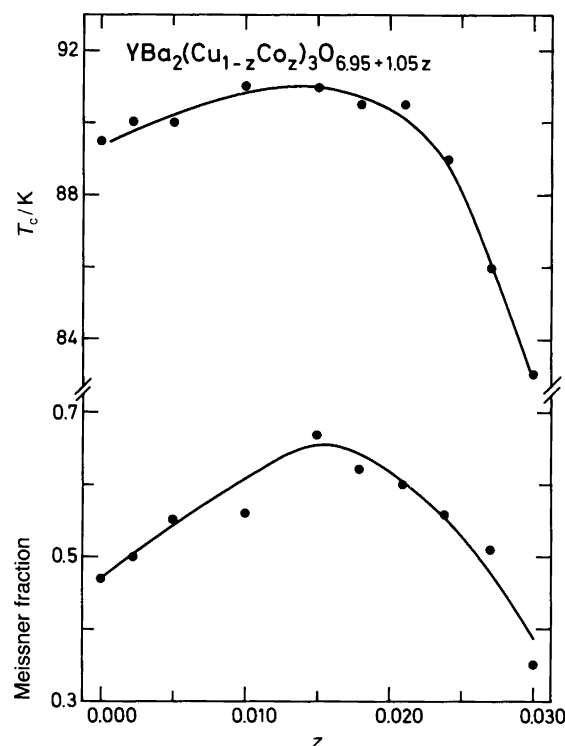


Fig. 5. Variation in  $T_c$  and Meissner fraction for  $\text{YBa}_2(\text{Cu}_{1-z}\text{Co}_z)_3\text{O}_{6.95+1.05z}$ ;  $0.000 \leq z \leq 0.030$ .

However, since such primary variables are not accessible, a correlation is sought in secondary variables such as: (i) structural properties (more specifically Cu–O coordination, bond distances, short-range order for oxygen vacancies etc., or more roughly the unit cell metric), (ii) the average electronic structure at the Cu site (more specifically, the removal of degeneration of the 'non-bonding' 3d Cu orbitals, the position of Fermi level relative to 2p oxygen levels) and (iii) properties related to the charge carriers (hole concentrations at particular Cu sites or the presence of hole-trapping, i.e. further oxidizable atoms).

For a discussion of the suppression of  $T_c$  with changes in the unit cell metric, two parameters describing structural distortions are introduced: (i) The *orthorhombic distortion*,  $D_o = (b/a) - 1$ , which (to some extent, see later) may serve as a gauge of the separation within the Cu–O chain and (ii) The *tetragonal deformation*,  $D_T = [2c/3(a+b)] - 1$ . For deformed octahedral or square-pyramidal coordination, an increase in  $D_T$  is a measure of increased splitting energy of the 'non-bonding' Cu 3d-orbitals.

For the substituted phases, there is no correlation between  $D_o$  and  $T_c$ .  $M = \text{Mg}$  and  $\text{Zn}$ , which have the largest effect on  $T_c$ , do not show decreased orthorhombic distortion. For  $\text{Zn}$ , the distortion is actually increased. The substituents  $\text{Li}$  and  $\text{Ni}$ , which have an intermediate effect on the orthorhombic distortion, affect  $T_c$  least.  $M = \text{Fe}$  and  $\text{Co}$ , which rapidly induce the tetragonal structure (as seen by PXD), corresponding to  $D_o = 0$ , suppress  $T_c$  rather



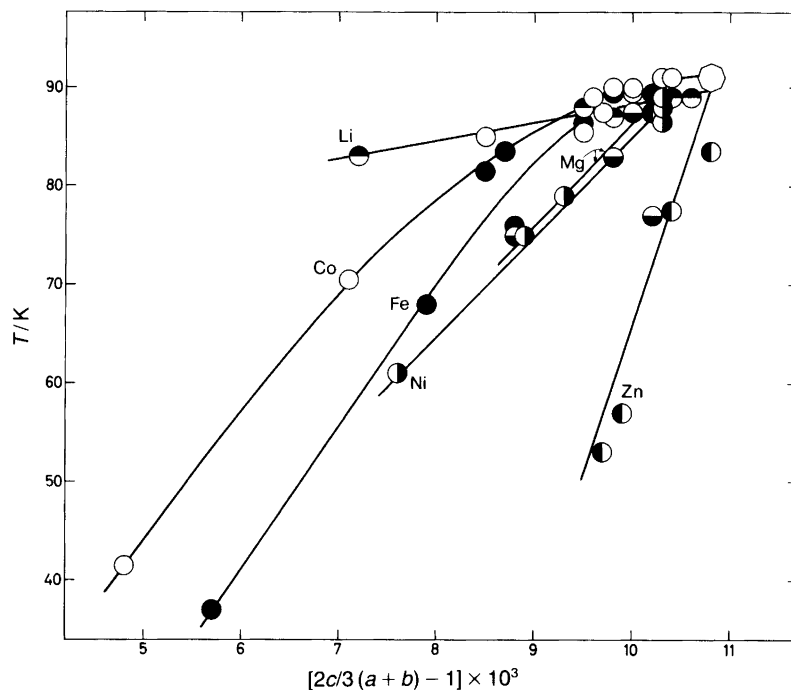


Fig. 6.  $T_c$  for oxygen-saturated  $\text{YBa}_2(\text{Cu}_{1-x}\text{M}_x)_3\text{O}_{9-\delta}$  as a function of the deformation parameter  $D_T = [2c/3(a+b) - 1]$ . The octagon refers to an unsubstituted sample, while the various metal substituents are distinguished by symbols. Least-squares fits are used when possible, otherwise curves are drawn as guides for the eye.

little, and remarkably, superconductivity coexists with the tetragonal structure over a wide composition range. However, it is possible that a short-range ordering of the vacancies in the twinned nanodomains may preserve a certain continuity of the Cu–O chains, even when the overall apparent symmetry is tetragonal. Such continuity is supposed<sup>65</sup> to be substantial for superconductivity to occur.

$D_T$  shows a distinct correlation with  $T_c$  for all these substituents (Fig. 6). It is also realized that the slight increase in  $T_c$  at the low substitution levels of  $M = \text{Co}$  is accompanied by an increase in  $D_T$ . The  $D_T$  versus  $T_c$  relationships are quantitatively different for the various substituents, which strongly suggests that other variables are also of importance. However, additional effects are believed to be of minor importance for  $M = \text{Li}$ , Fe and Co at low substitution levels, where  $\Delta T_c/\Delta D_T$  is small and comparable with those of Sr<sup>9</sup> and La<sup>8</sup> substitution for Ba. In this situation, Li, Fe and Co are believed to replace preferentially the square coordinated Cu(1) within the Cu–O chains.<sup>24,30,49,59,60</sup> At higher concentrations, Fe and Co act as efficient suppressors of superconductivity. A less detrimental effect for  $T_c$  is observed when the  $M$  occupancy at the Cu(2) site is increased [at the expense of the occupancy of the Cu(1) site] by firing the samples in a reducing atmosphere (with subsequent low-temperature reoxidation).<sup>59</sup> Apparently, Fe at the Cu(1) site interferes with charge transfer to the Cu(2) site, i.e. serves as a trap for mobile holes. A similar effect is ascribed to Pr at the Y site,<sup>66</sup> and may apply to the TlO layer in  $\text{YBa}_2\text{TlCu}_2\text{O}_7$ <sup>67</sup> or to the

$\text{PbCuO}_{2+x}$  assembly in (oxidized)  $\text{Pb}_2\text{Sr}_2(\text{Y,Ca})\text{Cu}_3\text{O}_{8+x}$ .<sup>68</sup> What Pr, Tl and Pb in these examples have in common is their mixed valency state, reached in the oxidative environment of the oxidized sample. This opens up the possibility of internal redox reactions, which in turn may interfere with the hole–phonon coupling, by (periodical) localization of the hole charges that otherwise would be transferred to the Cu(2) pairing centre.

The most rapid suppression of  $T_c$  is associated with  $M = \text{Ni}$ , Zn and Mg, which replace the square-pyramidally coordinated Cu(2) in the Cu–O sheets.<sup>48,61–63</sup> Zn is the most efficient suppressor of  $T_c$ , presumably through introduction of a large proportion of the strongly localized  $d^{10}$  state at the Cu(2) site, while keeping the effective hole concentration (as reflected in the Hall effect) virtually unchanged.<sup>69,70</sup>

The present experiments seem to support the commonly adopted view that the Cu–O pyramidal sheets are crucial for the superconductivity in cuprates, where they apparently serve as hole-pairing centres. As such, they are very sensitive to any alterations of the local electronic structure. The Cu–O chains are susceptible to the destruction of the superconductivity if an alteration occurs which is detrimental to their role as charge reservoirs.

The superconductivity is also sensitive to changes in the whole Cu–O structural assembly which reduce the tetragonal deformation of the Cu coordination octahedron, and in turn influence the energy difference between the partially filled Cu  $3d_{x^2-y^2}$  orbital and the other 'non-bonding'  $3d$  orbitals of Cu. A certain degree of solitary character of

the Cu  $3d_{x^2-y^2}$  orbital at the Fermi level (where it overlaps an O  $2p$  contributions) seems to be another prerequisite for superconductivity in the cuprates.

**Acknowledgement.** This work has received financial support from the Norwegian Council for Science and the Humanities (NAVF).

## References

- Karen, P., Fjellvåg, H., Braaten, O., Kjekshus, A. and Bratsberg, H. *Acta Chem. Scand.* **44** (1990) 994.
- Varadaraju, U. V., Natarajan, S., Kumar, T. S., Sampath, T. S., Paranthaman, M., Rao, G. V. S., Raju, N. P. and Srinivasan, R. *Physica B and C (Amsterdam)* **148** (1987) 417.
- Manthiram, A., Lee, S.-J. and Goodenough, J. B. *J. Solid State Chem.* **73** (1988) 278.
- Jirák, Z., Hejtmánek, J., Pollert, E., Triska, A. and Vašek, P. *Physica C (Amsterdam)* **156** (1988) 750.
- McCarron, E. M., Crawford, M. K. and Parise, J. B. *J. Solid State Chem.* **78** (1989) 192.
- Hor, P. H., Meng, R. L., Wang, Y. A., Gao, L., Huang, Z. J., Bechthold, J., Forster, K. and Chu, C. W. *Phys. Rev. Lett.* **58** (1987) 1891.
- Andresen, A. F., Fjellvåg, H., Karen, P. and Kjekshus, A. *Z. Crystallogr.* **185** (1988) A2.
- Karen, P., Fjellvåg, H., Kjekshus, A. and Andresen, A. F. *J. Solid State Chem.* **93** (1991). *In press.*
- Karen, P., Fjellvåg, H., Kjekshus, A. and Andresen, A. F. *J. Solid State Chem.* **93** (1991). *In press.*
- Karen, P., Fjellvåg, H. and Kjekshus, A. *J. Solid State Chem. To be published.*
- Saito, Y., Noji, T., Endo, A., Higuchi, N., Fujimoto, K., Oikawa, T., Hattori, A. and Furuse, K. *Physica B and C (Amsterdam)* **148** (1987) 336.
- Kirby, P. B., Harrison, M. R., Freeman, W. G., Samuel, I. and Haines, M. J. *Phys. Rev. B* **36** (1987) 8315.
- Siegrist, T., Schneemeyer, L. F., Wasczak, J. V., Singh, N. P., Opila, R. L., Batlogg, B., Rupp, L. W. and Murphy, D. W. *Phys. Rev. B* **36** (1987) 8365.
- Takabatake, T. and Ishikawa, M. *Solid State Commun.* **66** (1988) 413.
- Maeno, Y., Kato, M., Aoki, Y., Nojima, T. and Fujita, T. *Physica B (Amsterdam)* **148** (1987) 357.
- Hiratani, M., Ito, Y., Miyauchi, K. and Kudo, T. *Jpn. J. Appl. Phys.* **26** (1987) L1997.
- Mishra, N. C., Rajarajan, A. K., Patnaik, K., Vijayaraghavan, R. and Gupta, L. C. *Solid State Commun.* **75** (1990) 987.
- Youwen Xu, Sabatini, R. L., Moodenbaugh, A. R. and Suenaga, M. *Phys. Rev. B* **38** (1988) 7084.
- Gang Xiao, Cieplak, M. Z., Gavrin, A., Streitz, F. H., Bakshai, A. and Chien, C. L. *Rev. Solid State Sci.* **1** (1987) 323.
- Smith, M. G., Zhang, J. and Oesterreicher, H. *Mater. Res. Bull.* **23** (1988) 563.
- Jardim, R. F., Gama, S., De Lima, O. F. and Zacarelli, S. *Solid State Commun.* **68** (1988) 835.
- Kistenmacher, T. J., Bryden, W. A., Morgan, J. S., Moorjani, K., Du, Y. W., Qiu, Z. Q., Tang, H. and Walker, J. C. *Phys. Rev. B* **36** (1987) 8877.
- Ullmann, B., Heinemann, K., Krebs, H. U., Freyhardt, H. C. and Schwarzmann, E. *Physica C (Amsterdam)* **153-155** (1988) 872.
- Bordet, P., Hodeau, J. L., Strobel, P., Marezio, M. and Santoro, A. *Solid State Commun.* **66** (1988) 435.
- Jing, J., Bieg, J., Engelmann, H., Hsia, Y. and Gonser, U. *Solid State Commun.* **66** (1988) 727.
- Eibschütz, M., Lines, M. E., Tarascon, J. M. and Barbour, P. *Phys. Rev. B* **38** (1988) 2896.
- Dirken, M. W., Thiel, R. C., Smit, H. H. A. and Zandbergen, H. W. *Physica C (Amsterdam)* **156** (1988) 303.
- Shindo, D., Hiraga, K., Hirabayashi, M., Tokiwa, A., Kikuchi, M., Syono, Y., Nakatsu, O., Kobayashi, N., Muto, Y. and Aoyagi, E. *Jpn. J. Appl. Phys., Part 2*, **26** (1987) L1667.
- Sankawa, I., Sato, M. and Konaka, T. *Jpn. J. Appl. Phys., Part 2*, **27** (1988) L28.
- Kajitani, T., Kusaba, K., Kikuchi, M., Syono, Y. and Hirabayashi, M. *Jpn. J. Appl. Phys., Part 2*, **27** (1988) L354.
- Langen, J., Veit, M., Galfy, M., Jostardt, H.-D., Erle, A., Blumenröder, S., Schmidt, H. and Zirngiebl, E. *Solid State Commun.* **65** (1988) 973.
- Bringley, J. F., Chen, T.-M., Averill, B. A., Wong, K. M. and Poon, S. J. *Phys. Rev. B* **38** (1988) 2432.
- Kiemel, R., Schäfer, W., Kemmler-Sack, S., Kruschel, G. and Elschner, B. *J. Less-Common Met.* **143** (1988) L11.
- Maeno, Y., Nojima, T., Aoki, Y., Kato, M., Hoshino, K., Minami, A. and Fujita, T. *Jpn. J. Appl. Phys., Part 2*, **26** (1987) L774.
- Tarascon, J. M., Greene, L. H., McKinnon, W. R., Hull, G. W., Orlando, T. P., Delin, K. A., Foner, S. and McNiff, Jr., E. J. *Phys. Rev. B* **36** (1987) 8393.
- Zhu, Y., Suenaga, M., Xu, Y., Sabatini, R. L. and Moodenbaugh, A. R. *Appl. Phys. Lett.* **54** (1989) 374.
- Ferey, G., Le Bail, A., Laligant, Y., Hervieu, M., Raveau, B., Sulpice, A. and Tournier, R. *J. Solid State Chem.* **73** (1988) 610.
- Hepp, A. F., Gaier, J. R., Pouch, J. J. and Hamburger, P. D. *J. Solid State Chem.* **74** (1988) 433.
- Jayaram, B., Agarwal, S. K., Narasimha Rao, C. V. and Narlikar, A. V. *Phys. Rev. B* **38** (1988) 2903.
- Jee, Chan Soo, Nichols, D., Kebede, A., Rahman, S., Crow, J. E., Ponte Goncalves, A. M., Mihalisin, T., Myer, G. H., Perez, I., Salomon, R. E., Schlottmann, P., Bloom, S. H., Kuric, M. V., Yao, Y. S. and Guertin, R. P. *J. Supercond.* **1** (1988) 63.
- Oda, Y., Fujita, H., Omichi, T., Kohara, T., Nakada, I. and Asayama, K. *J. Phys. Soc. Jpn.* **57** (1988) 1548.
- Remschnig, K., Rogl, P., Eibler, R., Hilscher, G., Pillmayr, N., Kirchmayr, H. and Bauer, E. *Physica C (Amsterdam)* **153-155** (1988) 906.
- Bobtelsky, M. and Czosnek, S. *Z. Anorg. Allg. Chem.* **206** (1932) 113.
- Kirson, B. and Bobtelsky, M. *Bull. Soc. Chim. Fr.* **14** (1947) 560.
- Werner, P. E. *Program SCANPI*, Institute of Inorganic Chemistry, University of Stockholm, Sweden 1981.
- Ersson, N. O. *Program CELLKANT*, Chemical Institute, Uppsala University, Uppsala, Sweden 1981.
- Qian, M., Ma, Y., Ingalls, R., Sarikaya, M., Thiel, B., Kurosky, R., Han, C., Hutter, L. and Aksay, I. *Phys. Rev. B* **39** (1989) 9192.
- Gang Xiao, Cieplak, M. Z., Gavrin, A., Streitz, F. H., Bakshai, A. and Chien, C. L. *Phys. Rev. Lett.* **60** (1988) 1446.
- Miceli, P. F., Tarascon, J. M., Greene, L. H., Barbour, P., Rotella, F. J. and Jorgensen, J. D. *Phys. Rev. B* **37** (1988) 5932.
- Bhargava, S. C., Dorman, J. L., Jové, J., Gorochoy, O., Djega-Mariadassou, C., Pankowska, H. and Suryanarayanan, R. *J. Phys. C* **21** (1988) L905.
- Nishida, T., Ide, H., Maeda, Y., Nasu, H., Yagi, Y., Sakai, A. and Takashima, Y. *Bull. Chem. Soc. Jpn.* **62** (1989) 61.

52. Renevier, H., Hodeau, J. L., Bordet, P., Capponi, J. J., Marezio, M., Baudalet, F., Tolentino, H., Tourillon, G., Dartige, E., Fontaine, A., Martinez, J. C. and Prejean, J. J. *Physica C (Amsterdam)* 162-164 (1989) 51.
53. Adrian, F., *Phys. Rev. B* 38 (1988) 2426.
54. Dunlap, B. D., Jorgensen, J. D., Segre, C., Dwight, A. E., Matykiewicz, J. L., Lee, H. and Kimball, C. W. *Physica C (Amsterdam)* 158 (1989) 397.
55. Hiroi, Z., Takano, M., Takeda, Y., Kanno, R. and Bando, Y. *Jpn. J. Appl. Phys., Part 2*, 27 (1988) L580.
56. Le Dang, K., Renard, J. P., Vélú, E. and Laval, R. *Solid State Commun.* 72 (1989) 89.
57. Katsuyama, S., Ueda, Y. and Kosuge, K. *Matter. Res. Bull.* 24 (1989) 603.
58. Katsuyama, S., Ueda, Y. and Kosuge, K. *Physica C (Amsterdam)* 165 (1990) 404.
59. Smith, M. G., Taylor, R. D. and Oesterreicher, H. *Phys. Rev. B* 42 (1990) 4202.
60. Greaves, C., Slater, P. R. and Forgan, E. M. *Physica B (Amsterdam)* 156-157 (1989) 888.
61. Hangyo, M., Nakashima, S., Nishiuchi, M., Nii, K. and Mitsuishi, A. *Solid State Commun.* 67 (1988) 1171.
62. Maeda, H., Koizumi, A., Bamba, N., Takayama-Muromachi, E., Izumi, F., Asano, H., Shimizu, K., Moriwaki, H., Maruyama, H. and Kuroda, Y. *Physica C (Amsterdam)* 157 (1989) 483.
63. Shaked, H., Faber, J., Jr., Veal, B. W., Hitterman, R. L. and Paulikas, A. P. *Solid State Commun.* 75 (1990) 445.
64. Fjellvåg, H., Karen, P., Kjekshus, A., Kofstad, P. and Norby, T. *Acta Chem. Scand. A* 42 (1988) 178.
65. Jorgensen, J. D., Veal, B. W., Paulikas, A. P., Nowicki, L. J., Crabtree, G. W., Claus, H. and Kwok, W. K. *Phys. Rev. B* 41 (1990) 1863.
66. Fink, J., Nücker, N., Romberg, H., Alexander, M., Maple, M. B., Neumeier, J. J. and Allen, J. W. *Phys. Rev. B* 42 (1990) 4823.
67. Manako, T., Shimakawa, Y., Kubo, Y., Satoh, T. and Igarashi, H. *Physica C (Amsterdam)* 156 (1988) 315.
68. Cava, R. J., Batlogg, B., Krajewski, J. J., Rupp, L. W., Schneemeyer, L. F., Siegrist, T., van Dover, R. B., Peck, W. F., Jr., Gallagher, P. K., Glarum, S. H., Marshall, J. H., Farrow, R. C., Waszczak, J. V., Hull, R. and Trevor, P. *Nature (London)* 336 (1988) 211.
69. Terada, S., Kobayashi, N., Iwasaki, H., Tokiwa, A., Kikuchi, M., Syono, Y. and Muto, Y. *Preprint*.
70. Affronte, M., Pavuna, D., Martin, O., Licci, F., Besagni and Cattani, S. *Solid State Commun.* 70 (1989) 951.

Received January 21, 1991.